Macrophage polarization modulated by surface topography plays roles in calcium phosphate ceramics-instructed ectopic bone formation

Journal:	*ACS Applied Materials & Interfaces*
Manuscript ID	Draft
Manuscript Type:	Article
Date Submitted by the Author:	n/a
Complete List of Authors:	Li, Mingzheng; State Key Laboratory of Oral Diseases, West China Hospital of Stomatology, Sichuan University Guo, Xiaodong; State Key Laboratory of Oral Diseases, West China Hospital of Stomatology, Sichuan University Qi, Wenting; State Key Laboratory of Oral Diseases, West China Hospital of Stomatology, Sichuan University Bruijin, Joost.de.; Kuros Biosciences BV, Prof. Bronkhorstlaan Xiao, Yu; State Key Laboratory of Oral Diseases, Sichuan University, Bao, Chongyun; State Key Laboratory of Oral Diseases, West China Hospital of Stomatology, Sichuan University Yuan, Huipin; Kuros Biosciences BV, Prof. Bronkhorstlaan, MERLN Institute, Maastricht University

Macrophage polarization modulated by surface topography plays roles in calcium phosphate ceramics-instructed ectopic bone formation

Mingzheng Li[1#], Xiaodong Guo[1#], Wenting Qi[1], Joost D. de Bruijn[2], Yu Xiao[1], Chongyun Bao[1*], Huipin Yuan[2,3]*

1. State Key Laboratory of Oral Diseases, National Clinical Research Center for Oral Diseases, West China Hospital of Stomatology, Sichuan University, No.14, Section 3, Ren Min Nan Rd., Chengdu, 610041, Sichuan, China.

2. Kuros Biosciences BV, Prof. Bronkhorstlaan 10, 3723 MB Bilthoven, The Netherlands

3. MERLN Institute, Maastricht University, The Netherlands

* Corresponding authors: Yu Xiao, email: xiaoyu_8528@163.com, Tel: +86-028-85501233; Chongyun Bao, email: cybao9933@scu.edu.cn; fax: +86-28-85582167; tel: +86-028-85501233;.

# These two authors contributed equally to this work

KEYWORDS: macrophages polarization; material-instructed ectopic bone formation; submicron surface topography； micron surface topography; M1 macrophage； M2 macrophage

ABSTRACT

Macrophages are deemed as the crucial regulators of the early immune response after the implantation of materials. To investigate the roles of macrophages in ectopic bone formation instructed by calcium phosphate ceramics, two porous beta-tricalcium phosphate ceramics (β-TCP) with the same chemistry but various scale of surface topography, which were named as TCPs

(osteoinductive TCP with submicron surface topography) and TCPb (non-osteoinductive TCP with micron surface topography), were employed in this study. Depletion of macrophages with liposomal clodronate (LipClod) during the early stage of implantation blocked the bone formation in TCPs confirming the critical role of macrophages in material-instructed ectopic bone formation. Macrophage cells (i.e. RAW 264.7) cultured on TCPs in vitro were more likely to polarize toward M2 macrophages as evidenced by phenotypic markers and cytokine production, while RAW 264.7 cells on TCPb were M1 macrophage-like. Furthermore, such polarization of macrophages on ceramics was achieved by surface topography, since the distinct macrophages polarization was not seen in the indirect culture system. Moreover, it turned out that submicron surface topography directed macrophages polarization via PI3K/Akt pathway with the synergistic regulation of integrin β1. Finally, the M2 macrophage polarization on TCPs caused proper immune environment, leading to enhanced proliferation and osteogenic differentiation of mouse bone marrow-derived mesenchymal stem cells (mBMSCs) in vitro. At early implantation in FVB mice, TCPs recruited more macrophages than TCPb and with the increase of implantation time, TCPs favored M2 macrophage formation. The overall results suggest that submicron surface topography is favorable for macrophage recruitment and directs M2 macrophage polarization resulting proper immune environment to enhance bone formation.

1. Introduction

Multiple kinds of biomaterials have been developed to achieve bone regeneration, such as calcium phosphate (CaP) ceramics, titanium, polymers etc.[1] Among them, a group of osteoinductive materials, which has the capability to instruct new bone formation at ectopic sites, has shown a promising clinical application prospect in repairing bone defects with overcoming the complications caused by traditional autograft or xneograft.[2-3] Osteoinductive CaP ceramics could

not only accelerate bone formation, what's more, they were also available for the repair of critical-sized bone defects.[4-5] Furtherly, a previous study showed that an osteoinductive tricalcium phosphate (TCP) ceramic was equally efficient in bone repair as autologous bone grafts as well as collagen loaded with recombinant human bone morphogenetic protein 2 (rhBMP-2) in a sheep critical bone defects model,[6] which may be the best evidence for clinical relevance of osteoinductive CaP ceramics.

As generally accepted, the surface topography of CaP ceramics is the key factor in determining its osteoinductivity potential.[7-8] Unfortunately, so far the underlying mechanism of intrinsic osteoinduction or material-instructed ectopic bone formation is still a matter of controversy. Some researchers announced that material with different surface topography could result in different protein adsorption process, which was likely to elicit different recruitment, proliferation and differentiation behavior of stem cells.[9] Other researches have pointed out that particular surface topography could directly stimulate the osteogenic differentiation of stem cells and finally result in ectopic bone formation.[10] However, it is worth noting that those above researches merely focused on the relationship between surface topography and cells that directly related to osteogenesis, such as osteoblasts and mesenchymal stem cells, but lost the sight of the possible influence of surface topography on other cell types. As we now realized that bone formation is not simply relied on the skeletal system, but also orchestrated by the combined efforts of immune systems.[11] In fact, it is well known that the biomaterials will firstly contact with the immune cells (such as monocytes and macrophages) rather than osteoblasts or stem cells after implantation, and then start with the inflammation stage.[12]

In recent years, the concept that immune response is vital to the biomaterial-mediated bone regeneration has emerged,[11, 13] increasing evidence suggests that host immune responses after

biomaterials implantation could determine the fate of biomaterials in bone regeneration.[14] Of all the immune cells, macrophages, belonging to the innate immune response, are one of the first cells that contact with the materials,[15] and have been the main research focus due to their critical roles in bone formation and high plasticity in response to surrounding microenvironment.[12, 16] According to different stimuli, macrophages can be divided into two polarization phenotypes named classical pro-inflammatory macrophages (M1 macrophages) and alternative pro-healing macrophages (M2 macrophages).[17-18] In particular, M1 with the typical markers C-C chemokine receptor type 7 (CCR7) and inducible nitric oxide synthase (iNOS) can secrete inflammatory cytokines such as tumor necrosis factor-α (TNF-α), interleukin (IL) -6 and IL-1β. On contrast, M2 with the typical markers cluster of differentiation 206 (CD206) and arginase-1 (Arg-1) can yield the growth factors like vascular endothelial growth factor (VEGF) and insulin-like growth factor-1 (IGF-1),[19-22] which bear positive contributions in bone formation. It has been demonstrated that orthotopic bone formation was inhibited via depletion of osteomacs in bone injury model.[23-24] However, the biological mechanism of how macrophages interact with implanted CaP ceramic in ectopic bone formation remains to be addressed.

Considering the critical role of macrophages in orthotopic bone formation, we hypothesis that macrophages play a crucial role in material-instructed ectopic bone formation and the surface topography of osteoinductive materials could regulate the polarization behaviors of macrophages and functionally contribute to ectopic bone formation.

To verify the above assumption, two TCP ceramics with the same chemistry but various scale of surface topography and distinct osteoinductivity were employed in this study. Firstly, to explore the role of macrophages in material-instructed ectopic bone formation, TCPs (osteoinductive TCP ceramic with submicron surface topography) and TCPb (non-osteoinductive TCP ceramic with

micron surface topography) were implanted subcutaneously in FVB mice for 8 weeks and liposomal clodronate (LipClod) were applied during the early stage of implantation to deplete the macrophages. After that, the material-instructed ectopic bone formation was respectively evaluated. In addition, the specific markers of macrophages phenotypes and their secreted cytokines stimulated by TCPs and TCPb were respectively analyzed in vivo and in vitro (RAW 264.7 cells were used for in vitro study), and the related signaling pathways of macrophages polarization were then investigated. Meanwhile, the effect of the activated macrophages stimulated by TCPs and TCPb on the proliferation, migration and differentiation of mBMSCs was analyzed. This study will provide a promising alternative strategy to verify the osteoinductivity of materials during early stage after implantation and may contribute to the design of "smart biomaterials" with immunoregulatory function and advanced osteoinductivity.

2. Materials and Methods

The schematic diagrams of main evaluation process and key markers are shown in scheme.1, detailed information is described as follows:

2.1 Materials

Porous TCPs and TCPb were provided by Kuros Biosciences BV, the Netherlands, in both cubic form (4 x 4 x 4 mm) and disc form (ϕ14 x 2 mm). Preparation of the materials was described in details in previous report[10] and the main physicochemical properties of the materials were cited in Table 2 and surface morphology was shown in Figure 1a and b (section 3.1).

2.2 In vitro studies

Cells and culture

Cells. Murine monocyte/macrophage cell line RAW264.7 cells and mBMSCs (D1, CRL-12424) were purchased from ATCC and maintained in growth medium (GM) consisting of Dulbeccos

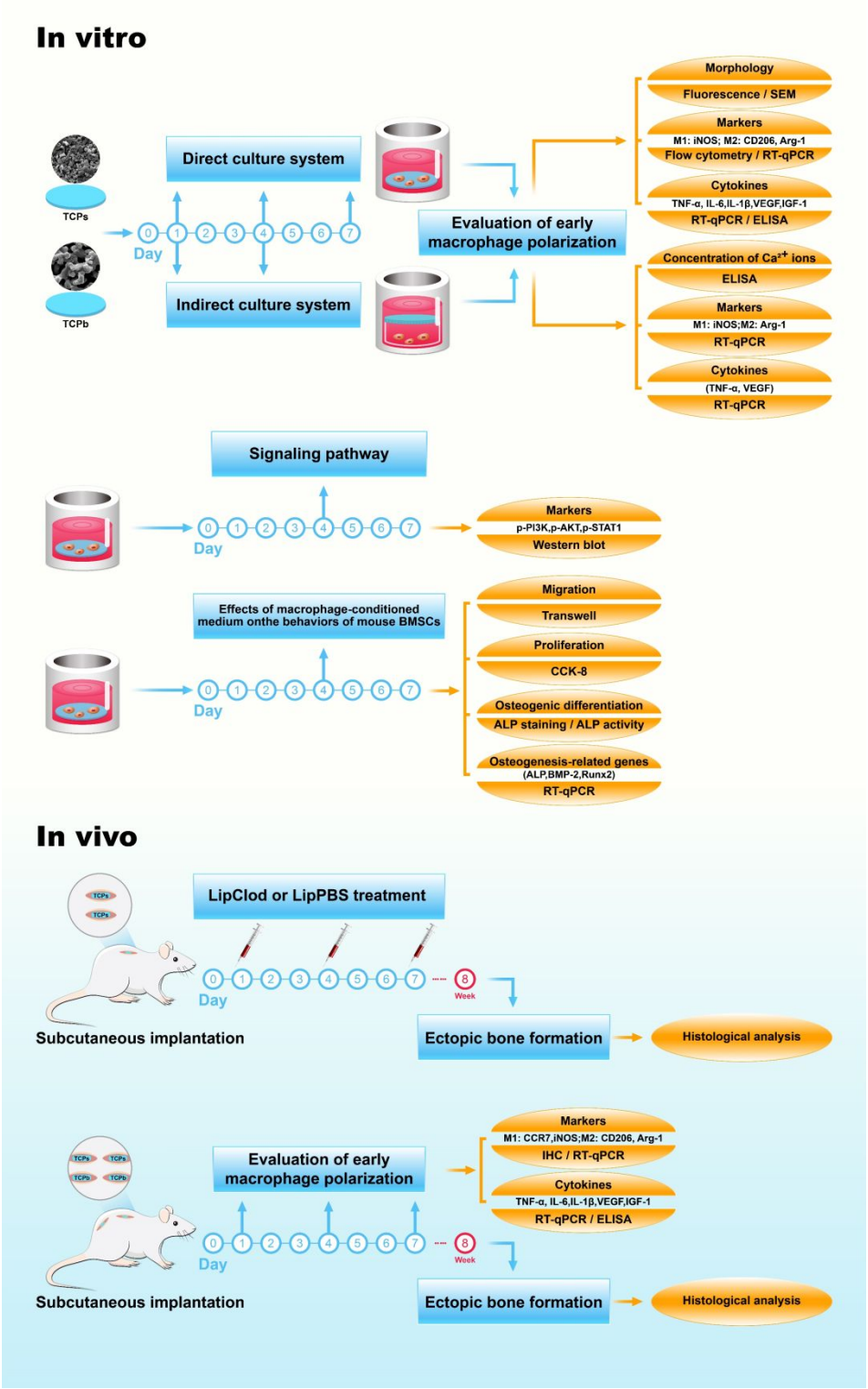

Scheme 1. Schematic diagrams of in vitro and in vivo experimental process

modified eagle medium (DMEM, Gibco, USA) supplemented with 10% fetal bovine serum (FBS, Gibco, USA), and 1% (v/v) penicillin/streptomycin (Hyclone, USA) at 37 °C in humidified atmosphere with 5% CO_2. RAW 264.7 cells and mBMSCs were harvested at 80%-90% confluence using a cell scraper and 0.25% trypsin/EDTA (Gibco, USA) respectively for further uses.

Direct culture of RAW 264.7 cells on TCP ceramics. Ceramic discs (ϕ14 x 2 mm) were placed in a 24-well plate (one sample per well) and soaked in 1 mL of GM for 24 h before cell seeding. After removing the medium, RAW 264.7 cells were seeded in 1 mL culture medium per well and allowed the cells to seed in 1h, then 1 mL medium was added, and the cells were finally cultured with the refreshments of culture medium every 2-3 days. The seeding densities of cells varied, with a cell density of $1x10^5$ cells/mL for flow cytometry assay, quantitative real-time polymerase chain reaction assay (RT-qPCR), enzyme-linked immunosorbent assay (ELISA) and Western blot (WB) and with a cell density of $2x10^4$ cells/mL for fluorescence staining and scanning electronic microscope (SEM) observation of the cells on ceramics. Supernatants at the seeding density of $1x10^5$ cells/sample were collected before medium refreshment, centrifuged at 3000 rpm for 10 minutes, mixed with normal GM at a ratio of 1:2 as conditioned media, which were stored at −80 °C until use.

Indirect culture of RAW 264.7 cells without the contact of ceramics. An indirect culture system (Fig. 5a) was designed to keep all other settings the same as in direct culture but seeded the cells on culture plate without contact of ceramic discs. The representative macrophages polarization-related genes and the concentration of Ca^{2+} ions were then evaluated.

Trans-well culture of mBMSCs with condition medium. A 24-well trans-well system (Corning, USA) was employed to mBMSC migration. Briefly, mBMSCs in serum free DMEM were seeded in the upper chamber at a density of $5x10^4$ cells per well, condition media were added in the bottom

chamber. After incubation for 24 h at 37 °C, nuclei of cells that migrated to the lower chamber were stained with DAPI and counted by the ImageJ software.

Culture mBMSCs with conditioned media. For the analysis of proliferation behavior, mBMSCs were seeded in a 96-well culture plate at a density of 2×10^3 cells per well. After 24 h of incubation, the medium was replaced by conditioned media and cultured for 1 d and 4 d, respectively. For the analysis of osteogenic differentiation of mBMSCs, the cells were seeded in a 24-well culture plate at a density of $5x10^4$ cells per well for alkaline phosphatase (ALP) activity ALP staining and RT-qPCR analysis. 24 hours later, the medium was refreshed by conditioned media and cultured for 7 days with the medium refreshed every 2-3 days.

Evaluations

SEM. The samples were dehydrated in ethanol with graded concentrations (30, 50, 70, 80 90, 95, 100% (v/v)) and gold-spattered for SEM observation (SEM, XL30 ESEM FEG, Philips, The Netherlands).

Fluorescent staining. Samples were rinsed with PBS, fixed in paraformaldehyde (4%) at 4 °C overnight, F-actin was stained by rhodamine-phalloidin (Sigma-Aldrich, Germany) and nuclei was stained with DAPI (Sloarbio, China) respectively according to the manufactures' protocol for fluorescent microscopic observation (FM, IX71, Olympus, Japan).

Flow cytometry assay. Cells were harvested with 0.25% trypsin/EDTA (Gibco, USA) and washed in PBS with centrifuge, then permeabilized with a Foxp3 buffer (Foxp3 / Transcription Factor Staining Buffer Set, eBioscience™) at 4°C for 60 min. Following the manufacturer's instructions, cells were incubated with monoclonal antibodies at 4°C for 40 min. Signals were detected with a flow cytometer (Bio-Rad, ZE5) and data was analyzed using Kaluza software. CD206 monoclonal antibody (0.125 μg/test, 12-2061-80, PE, eBioscience™) and iNOS monoclonal antibody (0.06

μg/test, 53-5920-82, Alexa Fluor 488, eBioscience™) were used and in each group, 4 replicas were included (n = 4).

RT-qPCR. Total RNA of samples was isolated by TRIzol (Thermo Fisher Scientific, USA), cDNA was subsequently acquired using the RevertAid First Strand cDNA Synthesis Kit (Thermo Fisher Scientific, USA). Real-time PCR reaction was proceeded at 95℃ for 10 min, followed by 95°C for 30 s, 60°C for 1 min and 72°C for 1 min for 40 cycles. Gene expressions were then measured using the ABI StepOnePlus™ Real-Time PCR System. GAPDH was chosen as the housekeeping gene for normalization, genes of iNOS, TNF-α, IL-6, IL-1β, Arg-1, VEGF, IGF-1, runt-related transcription factor 2 (Runx2), ALP and bone morphogenetic protein-2 (BMP-2) were targeted in this study and their primer sequences were listed in Table. 1. For each gene, 4 samples were used (n = 4) and each sample was performed in triplicate. Gene expression was calculated with $2^{-\Delta\Delta Ct}$ method.

ELISA. ELISA was applied for supernatant of in vitro cell culture. Supernatants of in vitro cell culture were harvested, centrifuged at 3000 rpm for 10 mins and kept at -80°C before use. ELISA assays of TNF-α, IL-6, IL-1β, VEGF and IGF-1 were conducted with commercial kits (Multiscience, China), following the manufacturer's instructions. 4 samples were used for each group (n = 4)

Western Blot (WB) assay. Samples with cells were lysed by RIPA buffer (Beyotime, Shanghai, China). After the total protein concentration was quantified by BCA assay using a Pierce™ BCA Protein Assay Kit (Thermo Fisher Scientific, USA), proteins in the lysates were denatured, separated by standard SDS-PAGE and then transferred onto a PVDF membrane. After being blocked in 5% BSA, the membranes were incubated with primary antibodies against Integrin β1

Table 1. Primer pairs used in the RT-qPCR

Genes		Primer sequences
iNOS	Forward	5'-CACCTTGGAAGAGGAGCAACTAC-3'
	Reverse	5'-GAGCAAAGGCGCAGAACTGA-3'
TNF-α	Forward	5'-CCCTCACACTCACAAACCACC-3'
	Reverse	5'-CTTTGAGATCCATGCCGTTG-3'
IL-6	Forward	5'-TTCTTGGGACTGATGCTGGTG-3'
	Reverse	5'-GCCATTGCACAACTCTTTTCTC-3'
IL-1β	Forward	5'-GCATCCAGCTTCAAATCTCGC-3'
	Reverse	5'-TGTTCATCTCGGAGCCTGTAGTG-3'
Arg-1	Forward	5'-ATCAACACTCCCCTGACAACCA-3'
	Reverse	5'-TTCCATCACCTTGCCAATCC-3'
VEGF	Forward	5'-AGGAGTACCCCGACGAGATAGA-3'
	Reverse	5'-CACATCTGCTGTGCTGTAGGAA-3'
IGF-1	Forward	5'-GGTGGATGCTCTTCAGTTCGTG-3'
	Reverse	5'-TGCTTTTGTAGGCTTCAGTGGG-3'
CD206	Forward	5'-CAGGAGGACTGCGTGGTTATG-3'
	Reverse	5'-GGTTTGCATCAGTGAAGGTGG-3'
CCR7	Forward	5'-ATCATTGCCGTGGTGGTAGTC-3'
	Reverse	5'-CTATTGGTGATGTTGAAGTTGGC-3'
Runx2	Forward	5'-AGCGGACGAGGCAAGAGTTT-3'
	Reverse	5'-AGGCGGGACACCTACTCTCATA-3'
ALP	Forward	5'-GGCACCTGCCTTACCAACTCT-3'
	Reverse	5'-GTTGTGGTGTAGCTGGCCCTTA-3'
BMP-2	Forward	5'-CGAATTTGAGTTGAGGCTGCTC-3'
	Reverse	5'-GCCGTTTTCCCACTCATCTCT-3'
GAPDH	Forward	5'-CCTCGTCCCGTAGACAAAATG-3'
	Reverse	5'-TGAGGTCAATGAAGGGGTCGT-3'

(1:2000, ab179471, abcam, UK), PI3K (4292, 1:1000, Cell Signaling Technology, USA), p-PI3K (4228, 1:1000, Cell Signaling Technology, USA), and AKT (4691, 1:1000, Cell Signaling Technology, USA), p-AKT (2965, 1:1000, Cell Signaling Technology, USA), STAT1 (ab47425, 1:500, abcam, UK), p-STAT1 (ab29045, 1:1000, abcam, UK) overnight at 4°C. β-Actin (ab8226, 1:1000, abcam, UK) was used as a loading control. After washed three times in TBS-Tween buffer, the membranes were incubated with HRP conjugated secondary antibodies (Beyotime, Shanghai, China) for 1 h at room temperature. The protein bands were visualized using

electrochemiluminescence (ECL) solution, and the relative intensity was quantified using AlphaEaseFC software (Alpha Innotech). Four samples were used for each group (n = 4).

Ion assay. Changes of calcium concentration in the indirect culture system were monitored using a QuantiChrom Calcium assay Kit (BioAssay Systems, Hayward, USA).

Cell Counting Kit-8 assay. A Cell Counting Kit-8 assay (CCK-8) kit (Dojindo, Japan) was used to evaluate the proliferation activity of cells. Absorbance at 450nm was measured with a spectrometer (Thermo Scientific, USA).

ALP staining. Cells were rinsed with PBS, fixed in paraformalde (4%) at 37°C for 30 mins. ALP staining was performed using a BCIP/NBT Alkaline Phosphatase Color Development Kit (Beyotime, Shanghai, China).

ALP activity. Cells were rinsed with PBS and lysed by RIPA buffer (Beyotime, Shanghai, China) after 7 d of culture, and the ALP activity were quantified using an ALP assay kit (Beyotime, Shanghai, China).

2.3 Animal experiment and sample evaluation

Animal experiments.

Subcutaneous implantation in FVB mice (male, 4-5 weeks old, obtained from Charles River Laboratory, Beijing, China) were used to evaluate the tissue responses of TCPs and TCPb. The mice were raised in temperature-controlled environment with artificial 12 h light/dark cycles and were fed with soft food diet. The ARRIVE guidelines and the Animal Care and Use Committee of Sichuan University Animal were strictly followed in animal experiments.

Surgical implantation. Surgical implantation was performed at sterile condition. After the mice were anaesthetized in order by inhalation of 2% isoflurane (ISOTHESIA, UK), intraperitoneal injection of ketamine (100 mg/kg, KetaVed, USA) and xylazine (16 mg/kg, AnaSed, USA),

buprenorphine (0.1 mg/kg, Buprenex Injection, USA) was subcutaneously injected for analgesia. Thereafter, either one or two subcutaneous pocket(s) was bilaterally created on the back, materials (in cubic form of 4x4x4mm) were inserted and the skin wound was closed with suture.

LipClod treatment. Once LipClod treatment was planned for the animals, 100 μL LipClod/pockect or 100 μL LipPBS (Vrijie Universiteit, Amesterdam) was locally injected in each pocket every 3 days starting from 1 d after surgery for 3 times.

Sample harvesting. Animals were sacrificed by cervical dislocation after general anesthesia at the time as planned. Implants were carefully harvested and processed accordingly for purposes.

Evaluation of the samples harvested

Histology. Both decalcified sections and non-decalcified section were made. The samples for non-decalcified sections were fixed in 4% paraformaldehyde, dehydrated in ethanol with gradient concentrations and then embedded in polymethyl methacrylate (Cool-Set A, Chengdu Aorigin, China). Non-decalcified sections (10-20 μm) were obtained with a diamond histological saw (SAT-001, Chengdu Aorigin, China) and stained with 1% methylene blue (Sigma-Aldrich, Germany) and 0.3% basic fuchsin (Sigma-Aldrich, Germany) solutions. For decalcified sections, the samples after fixation in 4% paraformaldehyde were refreshed with PBS solution (pH = 8) with 0.5 M EDTA and 0.5% paraformaldehyde once in 2-3 days for 2-3 weeks, then dehydrated in a series of gradient ethanol and finally embedded in paraffin. Decalcification solution was refreshed every 2-3 days and the whole decalcification Thin decalcified sections (4-7 μm) were obtained with (RM2016, Leica, Germany) and stained with Masson's trichrome or immunohistochemical staining as described below.

Immunohistochemistry. Paraffin-embedded decalcified sections were deparaffinized with xylene and ethanol, routine immunohistochemistry was performed as classically described.[25] The

following primary antibodies were applied in the study: F4/80 antibody (ab16911, 1:100, abcam, UK), CCR7 antibody (NB100–712, 1:50, Novus Biologicals, Littleton, CO, USA) and CD206 antibody (ab64693, 1:100, abcam, UK).

Histomorphometry. When histomorphometry was necessary, the sections were digitally scanned (Pannoramic DESK, P-MIDI, P250, 3D HISTECH) to images for analyses.

RT-qPCR. The obtained β-TCP implants were placed in RNAse/DNAse free tubes and stored at -80°C. Upon analysis, the samples were first thoroughly pulverized, then total RNA was isolated using TRIzol reagent. The gene expression of CCR7, iNOS, IL-6, TNF-α, IL-1β, CD206, Arg-1 and VEGF was analyzed by RT-qPCR assay following the protocols that described in Section 2.2.2. The primer sequences were listed in Table.1.

ELISA. The samples were immersed in 1% phenylmethylsulfonyl fluoride (PMSF) and thoroughly pulverized with ultrasonication for 5 min. The centrifugation at 12000 rpm was then proceeded for 10 min. Finally, the supernatants were harvested and ELISA assays for TNF-α, IL-6, IL-1β, VEGF and IGF-1 was performed with commercial kits (Multiscience, China) following the manufacturer's instructions.

2.4 Statistical analysis.

All data was analyzed by Graphpad Prism 6.0 using T test method and expressed as mean ± standard deviations (±SD). A probability value (p) of less than 0.05 was considered statistically significant.

3. Results

3.1 Bone formation in TCP ceramics following subcutaneous implantation in FVB mice

To study material-driven bone formation and the mechanism underneath, subcutaneous FVB mouse implantation model was established in-house and the bone forming abilities of the ceramics

were evaluated firstly. To do so, TCPb and TCPs were subcutaneously implanted in 10 FVB mice for 8 weeks. As histologically evaluated, bone was formed in 8/10 of TCPs explants and none of the 10 TCPb explants (Figure 1 and Table 2).

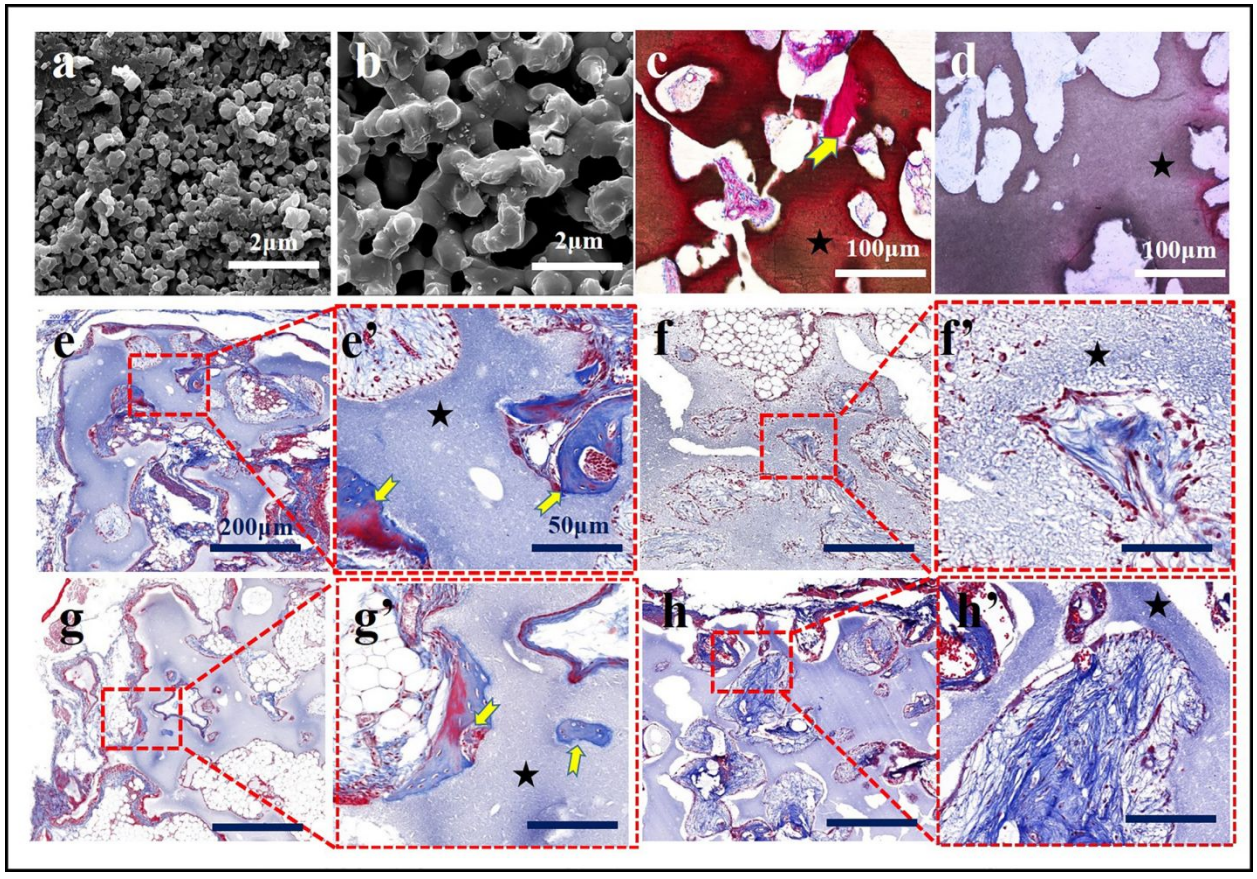

Figure 1. Surface morphology of TCPs (a) and TCPb (b) characterized by SEM. Histological staining of TCPs (c, e) and TCPb (d, f) after being implanted in vivo for 8 weeks, respectively. Histological staining of TCPs with local injection of LipPBS (g) and local injection of LipClod (h) after being implanted in vivo for 8 weeks respectively. The red dashed boxes (e', f', g', h') show the magnified regions of materials and regenerated tissues. In particular, black stars represent the residual materials and yellow arrows represent the newly formed bone.

3.2 Influence of LipClod on bone formation in TCPs

To verify the possible role of macrophages material-driven bone formation, local injection of LipClod was applied during the early stage of implantation to selectively deplete invading

macrophages. TCPs were implanted in 20 FVB mice for 8 weeks: 10 mice per group for local injection with LipClod and LipPBS (control group) respectively. No bone formation (0/10) was found in TCPs samples treated with LipClod (Table. 2 and Fig 1h, h'), however, new bone was histologically identified in almost all of the TCPs samples treated with LipPBS (7/10) (Table. 2 and Fig 1g, g').

Table. 2 Structure features and ectopic bone formation incidence rates of TCP ceramics

	TCPs	**TCPb**	**TCPs+LipClod**	**TCPs+LipPBS**
Average grain diameter (μm)	0.89±0.21	3.57±1.12	/	/
Average pore diameter (μm)	0.61±0.34	2.12±0.98	/	/
Ectopic bone formation incidence rate	8/10	0/10	0/10	7/10

3.3 Identification of the morphology of RAW 264.7 cells on TCPs and TCPb

After co-culture for 1 d, 4 d and 7 d, RAW 264.7 cells morphology on TCPs and TCPb ceramics was observed by SEM and FM. As shown in Fig.2, throughout the entire 7 days of incubation, the majority of RAW 264.7 cells on TCPs exhibited a relatively round shape. However, the cells on TCPb obviously presented elongated or irregular morphology with outstretched pseudopodia.

3.4 Effect of surface topography on macrophage polarization in the direct culture system

In order to investigate the surface topography on macrophages polarization in vitro, RAW 264.7 cells were directly cultured on TCPs and TCPb for 1 d, 4 d and 7 d. Then the results were

evaluated by flow cytometry, RT-qPCR and ELISA analysis respectively. To quantitatively verify the surface topography on macrophages polarization in vitro, the percentage of iNOS (M1 macrophages marker) positive and CD206 (M2 macrophages marker) positive cells were

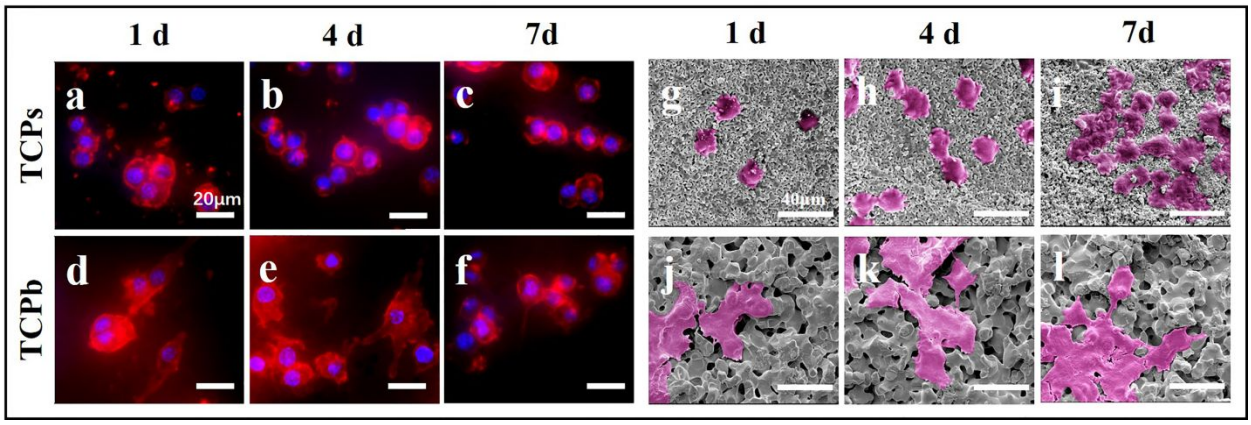

Figure 2. Morphology of RAW 264.7 cells cultured on TCPs or TCPb for 1, 4, and 7 days demonstrated by fluorescence staining (a to f) and SEM observation (g to l). For fluorescence staining, the cytoskeleton was stained in red with rhodamine phalloidin; the cell nuclei were stained in blue with DAPI. For SEM observation, the part of amaranth represents the seeded RAW 264.7 cells.

respectively measured by flow cytometry. Much more iNOS-positive cells could be detected on TCPb after 1 d of culture. However, there was no obvious change between TCPs and TCPb at 4 d and 7 d. Additionally, regardless of whether the cells cultured on TCPs or TCPb, the percentage of iNOS-positive cells peaked at day 1, followed by a significant decrease at day 4 and finally maintained at a relatively low level (Fig.3 a, c). An opposite variation trend was detected on the percentage of CD206-positive cells. The percentage of CD206-positive cells gradually increased over time and peaked at 7 d in both TCPs and TCPb groups. In particular, though less CD206-positive cells in TCPs group versus TCPb group at 1 d, more macrophages polarized into CD206-positive cell under the simulation of TCPs at 7 d, but no difference was found at 4 d (Fig.3 b, d).As shown in Fig.4a, RT-qPCR results showed that the expression of all the pro-inflammatory genes

(including iNOS, TNF-α, IL-6, and IL-1β) was promoted by TCPb versus TCPs at 1 d and 4 d. However, an interesting fact could be observed that the expression of iNOS, TNF-α and IL-1β showed no statistical difference between these two groups at 7 d. In addition, the expression of Arg-1, as a classical M2 intracellular marker, gradually down-regulated in response to TCPb, while

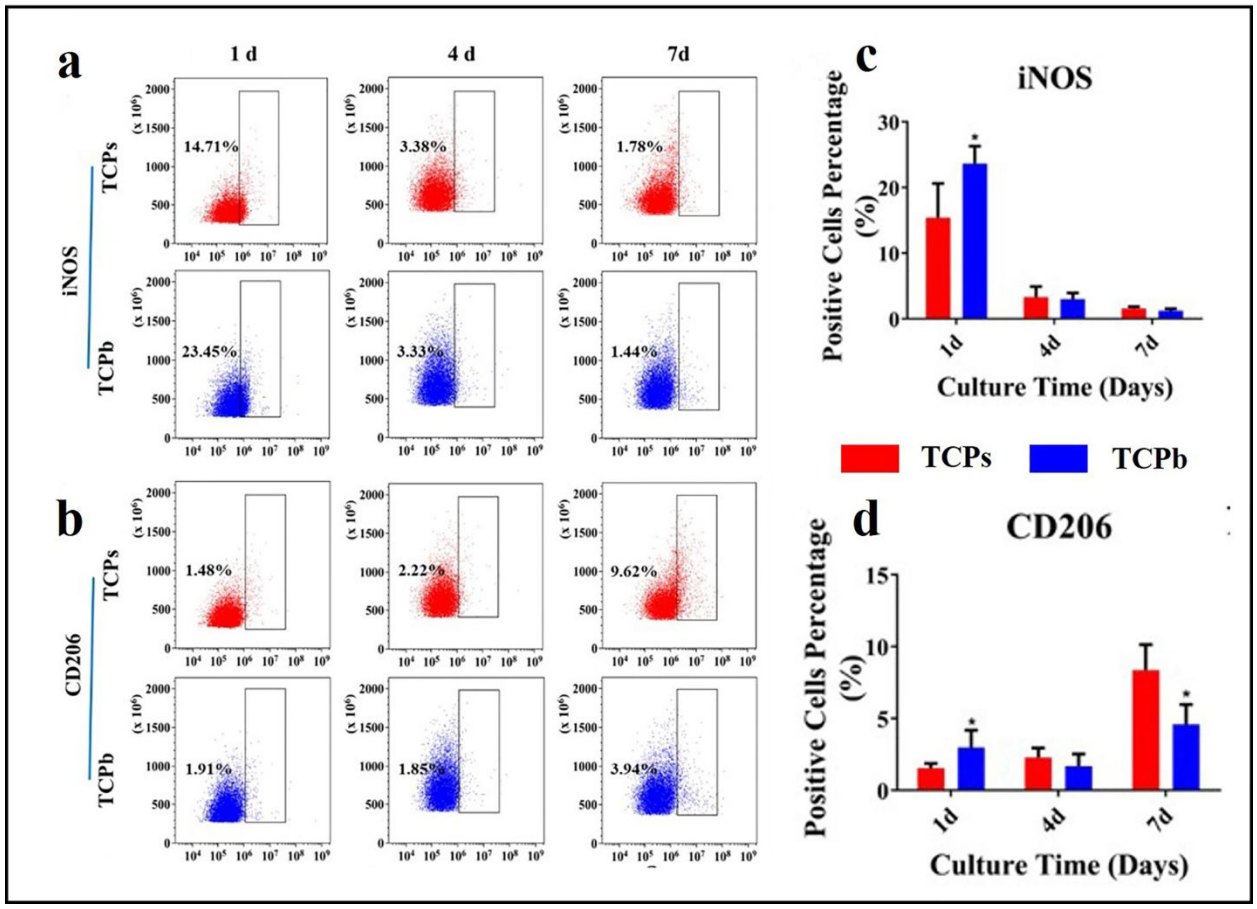

Figure 3. The percentages of iNOS (a) and CD206 (b) positive cells in RAW 264.7 cells cultured on TCPs and TCPb for 1, 4, and 7 days respectively analyzed by flow cytometry. (c) and (d) quantitatively summarized the percentage of iNOS or CD206 positive cells at each determined time point. The asterisk * in these charts and all of the following bar charts represents significant difference (p) between TCPb groups and TCPs groups. Specifically, * represents $p<0.05$; ** represents $p<0.005$, *** represents $p<0.0005$ and **** represents $p<0.00005$.

TCPs can elicit a gradual up-regulation trend along with time. Therefore, although TCPb possessed the highest Arg-1 expression level after 1 d, there was no notable difference between these two groups after 7 d of culture. The expression of pro-healing genes (including VEGF and IGF-1) was not significantly different between TCPs and TCPb at 1 d, however, higher expression of VEGF and IGF-1 was detected in TCPs group after 4 d and 7 d of culture compared with the TCPb group.

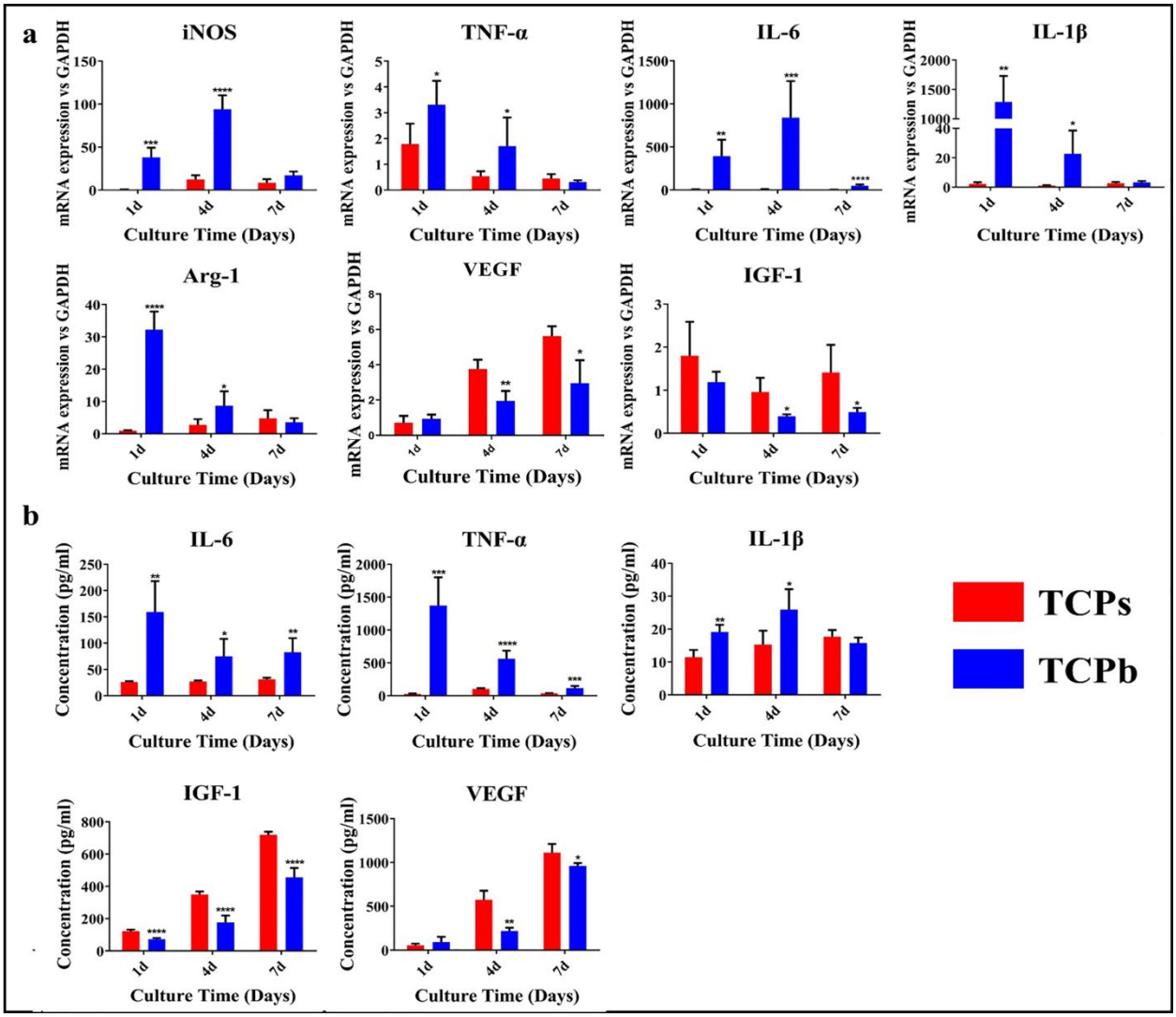

Figure 4. (a) The relative expression of pro-inflammatory genes, including iNOS, TNF-α, IL-6, and IL-1β and pro-healing genes, including Arg-1, VEGF and IGF-1 in RAW 264.7 cells cultured on TCPs and TCPb for 1, 4, and 7 days； (b) Inflammatory cytokines (IL-6, TNF-α, and IL-1β) and growth factors (VEGF and IGF-1) secreted by RAW 264.7 cells cultured on TCPs and TCPb for 1, 4, and 7 days.

ELISA analysis (Fig.4 b) showed analogous results with the genes expression. Firstly, significantly higher concentration of inflammatory cytokines (including IL-6, TNF-α) was detected in the TCPb group than the TCPs group at each time point. For IL-1β, TCPb enhanced its concentration at 1 d and 4 d, but no significant difference was observed at 7 d. On the other hand, for IGF-1, lower concentration level was detected on the TCPb group at each time point. The variation of VEGF's concentration was similar with IGF-1 at 4 d and 7 d, but no obvious difference was observed at 1 d.

3.5 The polarization of macrophages cultured in the indirect culture system

Except for the surface topography of materials, we also wanted to figure out if there was any other factor to influence the polarization process of RAW264.7 cells when they were cultured with TCPs or TCPb. To answer this question, an indirect culture system (Fig. 5a) was designed to separate the materials and cells. The results demonstrated that there was no pronounced distinction in the expression of related genes (iNOS and TNF-α as markers for M1 macrophages, Arg-1 and VEGF markers for M2 macrophages) between TCPs and TCPb group at1 d and 4 d (Fig. 5c). In particular, because of the important role of Ca^{2+} in macrophages polarization, the concentration of Ca^{2+} in the conditioned medium derived from the indirect culture system was evaluated in this study. Significant lower concentration of Ca^{2+} ions was detected in TCPs group compared with the TCPb group (Fig. 5b).

3.6 Investigation on the polarization mechanisms via WB assay

WB assay was proceeded in this study to explore the mechanism of macrophages polarization process on TCPs and TCPb. After co-culture with the ceramics for 4 days, the proteins in related signal pathways that could direct the polarization of macrophages were evaluated. The expression

levels of integrin β1, phosphorylation of PI3K and Akt were significantly higher on TCPs than that on TCPb, whereas phosphorylation of STAT1 was significantly enhanced by TCPb. (Fig.6 a,b)

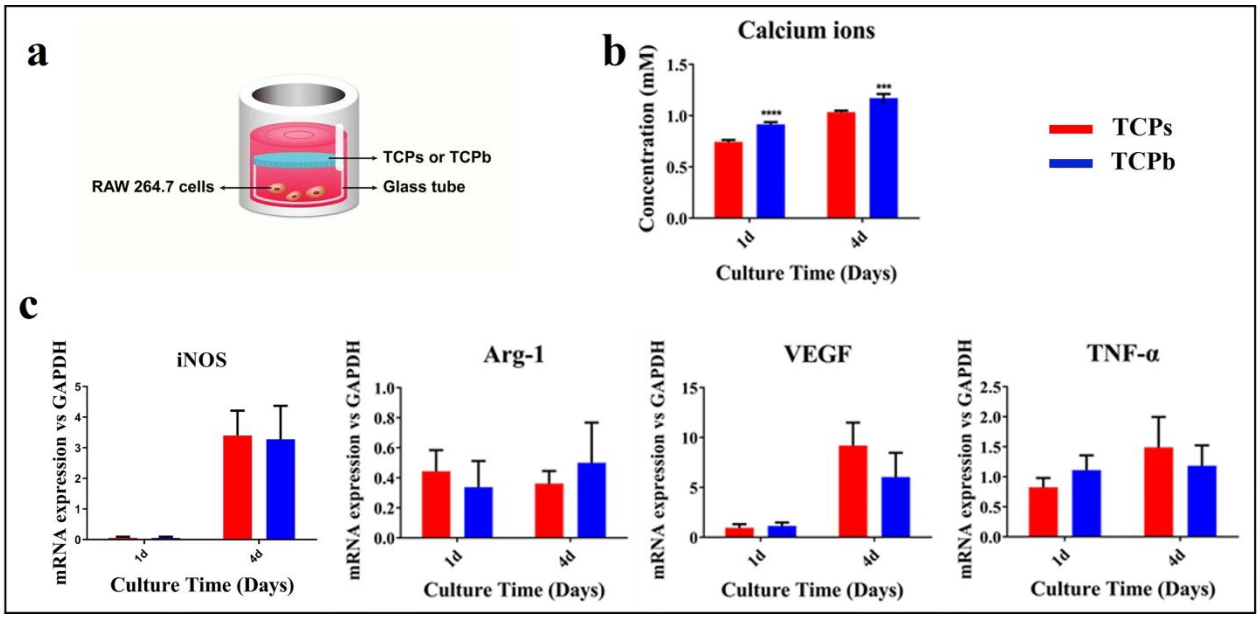

Fig. 5 (a) Schematic diagram of the indirect culture system; (b) The concentration of Ca^{2+} in TCPs and TCPb groups at 1 d and 4 d. (c) The expression of representative genes including iNOS, Arg-1, VEGF and TNF-α of RAW 264.7 cells cultured in the indirect culture system for 1 and 4 days.

3.7 Effects of macrophage-conditioned media on the proliferation, migration and osteogenic differentiation of mBMSCs in vitro

CCK-8 assay was performed to investigate the proliferation of mBMSCs cultured in various conditioned media. As shown in Fig. 7a, at each time point, the cells on the TCPs group exhibited significantly increased vitality compared with the TCPb group. The 24-well transwell system was employed to investigate the migration of mBMSCs cultured with various macrophage-conditioned media. However, for the migration of mBMSCs, FM images clearly identified that there was no significant difference between the two groups (Fig. 7b, c).

ALP has been used extensively as a marker of osteogenic differentiation of stem cells. The osteogenic differentiation of mBMSCs influenced by different conditioned media was then successively characterized via ALP staining and quantitative analysis of ALP activity. As shown in Fig. 7d, conditioned media derived from TCPs performed more pronounced effect to enhance the ALP activity in mBMSCs after cultured for 7days, which was confirmed by the results of ALP staining (Fig. 7f). Similarly, the expression of osteogenesis-related genes including BMP2 and ALP also up-regulated in the TCPs group in comparison with the TCPb group. However, there was no difference in the expression of Runx2 between the two groups (Fig. 7e).

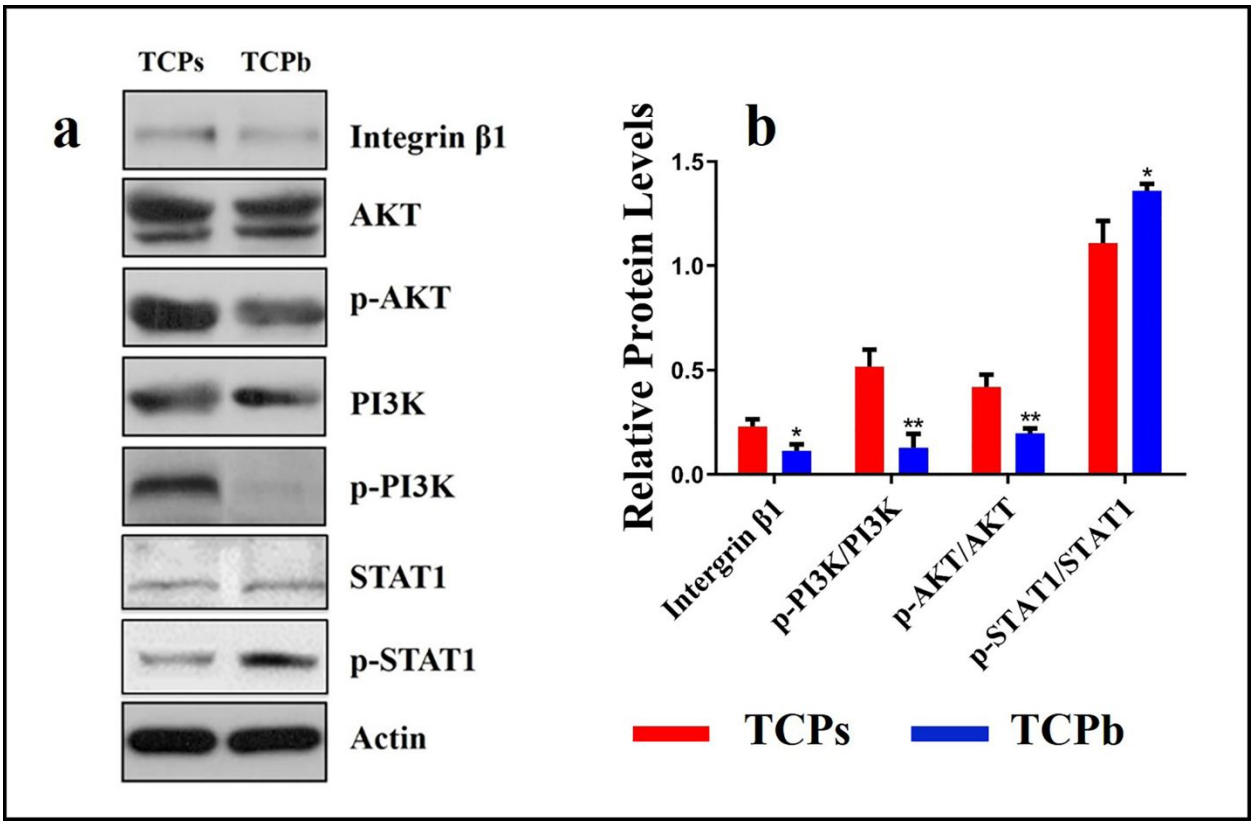

Figure 6. The protein levels of integrin β1 and phosphorylation of PI3K, AKT and STAT1 in RAW264.7 cells cultured on TCPs and TCPb respectively. (a) WB analysis of integrin β1, PI3K, p-PI3K, AKT, p-AKT, STAT1, and p-STAT1 in RAW 264.7 cells cultured on TCPs and TCPb for 4 days. (b) Quantification of the protein levels of integrin β1 and phosphorylation of PI3K, AKT and STAT1.

3.8 Macrophage polarization in ceramics at early implantation

In order to investigate the polarization of macrophages in vivo, ceramics were subcutaneously implanted in FVB mice for 1, 4 and 7 days, and the explants were evaluated with respect to immunohistochemical staining (Fig. 8), genes and protein expression (Fig.9). At each time point, 5 mice were used for immunohistochemistry analysis and 5 mice in total were used for RT-qPCR and ELISA analysis.

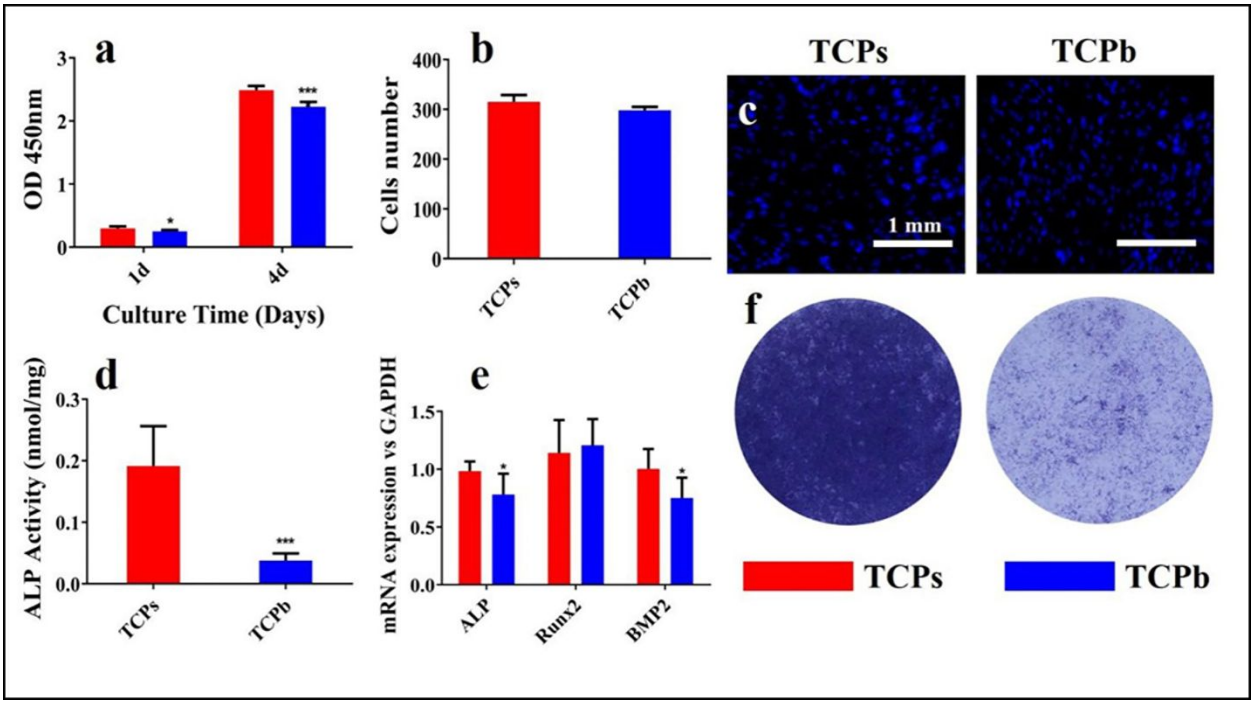

Figure 7. (a) The OD values obtained by CCK-8 assay to show the proliferation activity of mBMSCs after the cells were cultured in different CMs for 1 and 4 days; (b) The amount of cell nuclei that migrated to lower chamber after the cells were cultured in transwell system with different CMs for 1 day; The related FM images were shown in (c); (d) The ALP activity of mBMSCs after they were cultured in different CMs for 7 days. (e) The expression of genes including ALP, Runx2 and BMP2 after the cells were cultured in different CMs for 7 days; (f) ALP staining images of the mBMSCs after the cells were cultured in different CMs for 7 days.

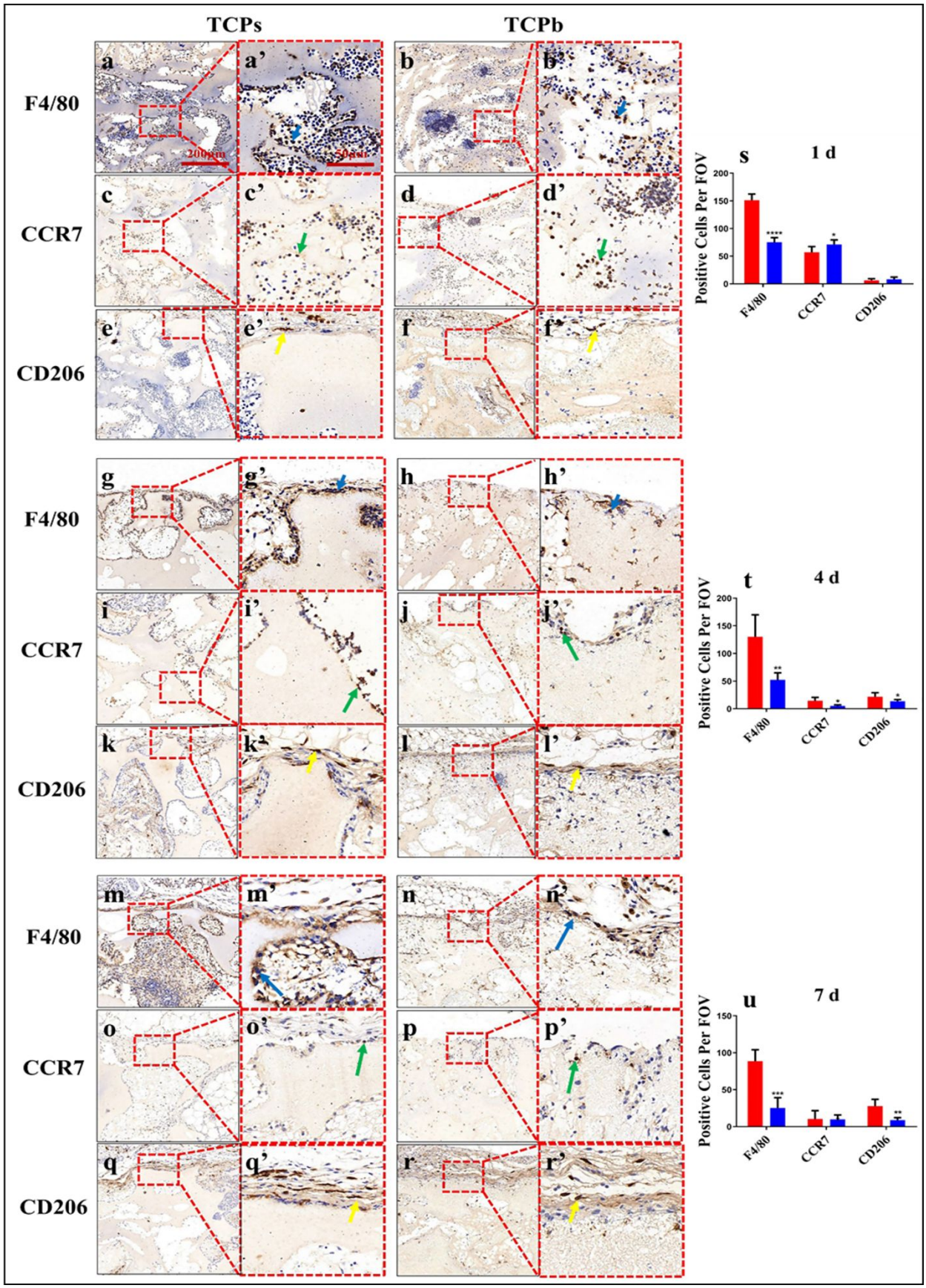
TCPs
TCPb
F4/80
CCR7
CD206
a
a'
b
b'
c
c'
d
d'
e
e'
f
f'
200μm
50μm
s
1 d
Positive Cells Per FOV
F4/80
CCR7
CD206
g
g'
h
h'
i
i'
j
j'
k
k'
l
l'
t
4 d
m
m'
n
n'
o
o'
p
p'
q
q'
r
r'
u
7 d

Figure 8. Immunohistochemistry staining of F4/80, CCR7 and CD206 positive cells after TCPs and TCPb were respectively implanted into the FVB mice for 1 (a to f'), 4 (g to l'), and 7 (m to r') days. Specifically, the red dashed boxes are the magnified staining regions and the blue arrows represent the F4/80 positive cells, green arrows represent the CCR7 positive cells, yellow arrows represent the CD206 positive cells. Images s, t and u quantitatively summarized the number of positive cells per field of view (FOV) at each determined time point.

3.8.1 Immunohistochemical staining

Immunohistochemical staining of F4/80, CCR7 and CD206 was applied to decalcified sections of TCPb and TCPs harvested at 1 d, 4 d and 7 d after implantation, followed by histomorphometrical assays regarding the positive cells in FOV. More F4/80-positive cells were observed in TCPs than TCP b at all time points (Fig. 8a-b', g-h', m-n', s-u).

Moreover, the number of CCR7-positive cells decreased sharply from day 1 to day 7, with more CCR7-positive cells on TCPb after 1 day of implantation (Fig.8c-d', s), but more on TCPs at 4 d (Fig. 8i-j', t). However, there was no difference between TCPs and TCPb at 7d (Fig. 8o-p', u).In addition, the number of CD206-positive cells increased with time in TCPb and TCPs, but TCPs had more CD206-positive cells than TCPb at day 4 and day 7(Fig. 8k-l', q-r', t, u). However, there was no obvious variation between TCPs and TCPb groups after 1 day of implantation (Fig. 8e-f', s).

3.8.2 Pro-inflammatory and pro-healing genes and proteins production

As shown in Fig. 9a, at 1 day after implantation, the expression of IL-6 and CCR7 significantly increased in the TCPb group versus the TCPs group. However, except for the up-regulation of CD206, there was no significant difference in other genes after 1day. Interestingly, the expression of almost all the M1 macrophages genes (iNOS, CCR7, IL-1β and TNF-α) was evidently up-regulated in the TCPs group compared with the TCPb group at 4 d after implantation, and this trend continued to 7 d for CCR7 and TNF-α. On the contrary, the expression of IL-6 and IL-1β in

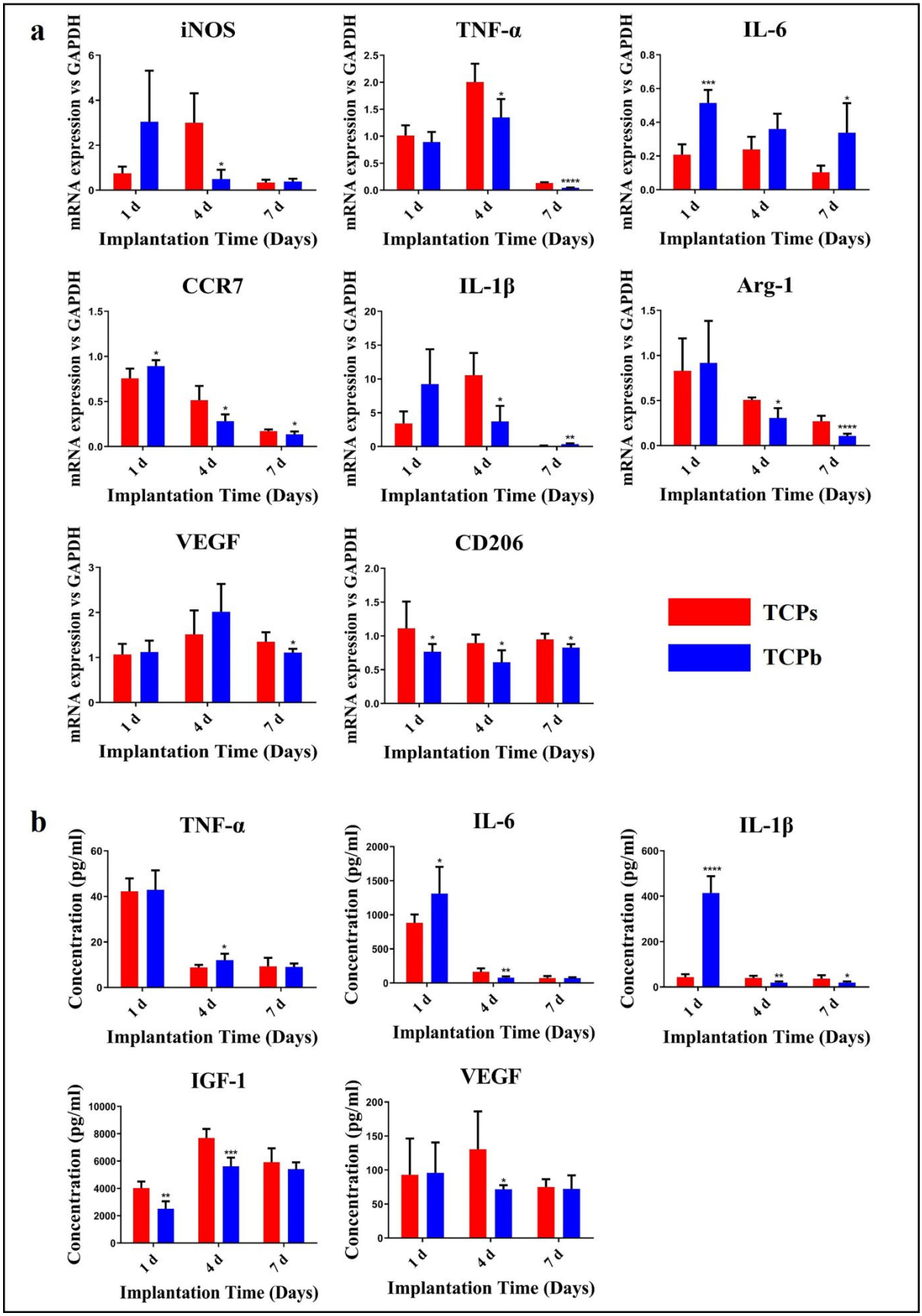
a
iNOS
TNF-α
IL-6
CCR7
IL-1β
Arg-1
VEGF
CD206
mRNA expression vs GAPDH
Implantation Time (Days)
1 d
4 d
7 d
TCPs
TCPb
b
TNF-α
IL-6
IL-1β
IGF-1
VEGF
Concentration (pg/ml)
Implantation Time (Days)

Figure 9. (a) The expression of pro-inflammatory genes including iNOS, TNF-α, IL-6, CCR7 and IL-1β and pro-healing genes including Arg-1, VEGF and CD206 after TCPs and TCPb were respectively implanted into the FVB mice for 1, 4, and 7 days, relative to housekeeping gene GAPDH；(b) The concentration of inflammatory cytokines (IL-6, TNF-α, and IL-1β) and growth factors (VEGF and IGF-1) after TCPs and TCPb were respectively implanted into the FVB mice for 1, 4, and 7 days.

the TCPs group showed down-regulated at 7 d, while no difference in the expression of iNOS was observed at 7 d. In terms of the M2 macrophage genes, it was noted that the expression of most M2 macrophages genes (Arg-1 and CD206) was obviously up-regulated in the TCPs group at 4 d and 7 d. In addition, the expression of VEGF showed no obvious change at 4 d but up-regulated in the TCPs group at 7 d.

The concentration of related proteins analyzed by ELISA was similar with the performance of genes expression (Fig. 9b). Except for TNF-α, the levels of inflammatory cytokines (IL-6 and IL-1β) were higher in the TCPb group compared with the TCPs group at 1 d. On the contrary, the levels of IL-6 and IL-1β showed opposite trend after 4 days of implantation. In addition, except for IL-1β, the levels of inflammatory cytokines (TNF-α and IL-6) showed no significant difference between TCPs and TCPb at 7 d. Similarly, it was noted that the levels of growth factors (VEGF and IGF-1) were higher in the TCPs group after 4 days of implantation. However, the differences disappeared at 7 d. Meanwhile, it should be noted that the levels of inflammatory cytokines exhibited a declined trend from 1 d to 7 d.

4. Discussion

Once the materials are implanted in the body, immune cells will migrate to the implanted biomaterials and trigger a series of host immune response. Previous studies have demonstrated the critical role of macrophages in regulation of immune response after biomaterials implantation.[14,

[26] Our investigations further revealed that macrophages were essential in material-instructed ectopic bone formation and macrophage polarization showed high sensitivity to the surface topography of osteoinductive materials, and this effect could form different immune environment during the early period which was pivotal in the process of ectopic bone formation.

LipClod is widely used in the experiments to investigate the role of macrophages in bone homeostasis and bone healing/repair. As an effective method, the function of LipClod on elimination of macrophages has been well validated by numerous studies.[23, 27] In our study, we found that depletion of macrophages with Lipclod during the early stage of implantation blocked the bone formation in TCPs confirming the indispensable role of macrophages in material-instructed ectopic bone formation. Meanwhile, in our study, more macrophages recruited on TCPs while fewer macrophages recruited on TCPb during the early stage of implantation. This result is consistent with Gamblin's research claiming that more macrophages could lead to more pronounced ectopic bone formation.[28] The above results suggest that macrophages in the early phases are participated and play an important role in material-instructed ectopic bone formation.

The change of cell morphology is an effective indicator to reflect the functional and differentiation status of macrophages.[29-31] Chen et al. demonstrated that the morphological changes of macrophages stimulated by different chemical and topographic cues strongly suggested the possible regulation of immune environment. Those studies have revealed that the physical cues including nanostructure and pore size on an alumina surface can regulate the prime macrophages to cells with elongated shape and finally accelerate the inflammatory reaction. Meanwhile, cells with round shape participated more in pro-healing process.[32] Pervious studies demonstrated that macrophages with elongated shape were considered M1 macrophages.[33-34] In our study, the results of FM and SEM proved that the stimulus derived from different surface topographies could result

in corresponding morphology changes of RAW 264.7 cells, with a relatively round shape on TCPs but irregular shape on TCPb. This phenomenon proved that β-TCP with different surface topography might provide distinct stimulus to the RAW 264.7 cells, resulting in different morphologies. Subsequent analysis indicated that there were less percentage of RAW 264.7 cells expressing M1 marker (iNOS) and more percentage of RAW 264.7 cells expressing M2 marker (CD206) in the TCPs group compared with that in the TCPs group. Furthermore, TCPs not only enhanced the release of growth factors but decreased the secretion of inflammatory cytokines. Thus, our present study revealed a similar result that the elongated or irregular cells on TCPb were likely to activate the pro-inflammatory response, whereas the round cells on TCPs exhibited pro-healing state. However, according to some previous reports, the researchers have pointed out that the macrophages with round shape were considered as M1 phenotype to enhance the pro-inflammation, while the macrophages with elongated shape were more involved in pro-healing process which could be defined as M2 phenotype.[31, 35] Therefore, the actual relationship between shape of macrophage and the correspondence phenotype is still not fully understood. Further investigations are required to clarify their comprehensive relationship.

In order to further verify the key role of surface topography in macrophages polarization, an indirect culture system was designed. The results showed that the expression of all genes showed no significant differences between TCPs and TCPb groups, reconfirming the importance of the surface topography in regulating the macrophages polarization. It should be noted that based on some previous studies, except for the physical cues, the concentration of Ca^{2+} in culture medium was regarded as another vital factor to regulate the macrophages behavior.[36] Fox example, Chen et al. have revealed that the pro-inflammatory genes such as IL-1β and IL-6 could be down-regulated via decreasing Ca^{2+} concentration, whereas the pro-healing genes including BMP-2, IL-

10 was up-regulated simultaneously.[37] However, in our study, although the concentration of Ca^{2+} was different from TCPs and TCPb groups at each time point, there was almost little impact on regulating the macrophages polarization. The reason of this phenomenon may be explained by the fact that the concentration of Ca^{2+} in our culture medium was too lower than that in Chen's study to provoke the cells. Taken together, these findings indicated that macrophages polarization could be modulated by the surface topography. Submicron surface topography of TCP will condition the immune microenvironment with the decreased inflammatory cytokines and increased growth factors by modulating macrophage polarization toward M2 phenotype while micron surface topography of TCP was prone to condition the immune microenvironment with excessive inflammatory cytokines by inducing macrophage polarization toward M1 phenotype.

In vivo studies were carried out to verify whether the in vitro experimental results of macrophage polarization in the evaluation system were consistent with the in vivo results, which would further verify the feasibility of designing better osteoinductive materials by controlling the surface topography to regulate the immune response. The results of in vivo from our current research showed a similar trend with that in vitro: more M1 cells were observed on TCPb samples and result in more pronounced pro-inflammatory effect at 1 d after implantation. Furthermore, TCPs could induce macrophage polarization toward M2 cells and result in more pronounced pro-healing effect. More intriguingly, more M1 cells existed on TCPs surface and the secretion of related inflammatory cytokines significantly increased in TCPs group after 4 d of implantation, which was contrary to the results in vitro. The reason could be summarized as follows: immunohistochemistry results showed the fact that TCPs could promote the recruitment of macrophages at each time point compared with TCPb groups, which may counteract the effect of surface topography on the polarization of macrophages toward M1 phenotype. Furthermore, it is

well known that in vivo microenvironment is far more complicated than the in vitro cell culture system, there are undoubtedly many other genes and proteins which also have considerable impact on the macrophages polarization.[38-39] It is worth noting that M1 cells and all inflammatory cytokines peaked at 1day after implantation, followed by a sharp decline, and remained relatively stable at 4d and 7d after implantation. It has been reported that M1 macrophages were mainly present in the first two days after the material implanted and secreted a large amount of the inflammatory factors in the acute stage, which is similar to our results.[40-41] Therefore, we speculate that M1 cells and inflammatory response may mainly play a major role at 1d after the implantation of the material rather than 4 d and 7d in our experiments.

After determining the immune environment produced by the interaction between macrophages and TCP with different surface topography, we further explored the role of different immune environment in osteogenesis. Evidence is accumulating that various cytokines secreted by macrophages contribute to bone formation.[18, 42] Previously published studies demonstrated that inflammatory cytokines secreted by M1, including IL-6, IL-1β and TNF-α, could bring negative effect on bone formation by inhibiting osteoblast activity and elevating osteoclast activity.[43-44] Besides, M2 macrophages could contribute to osteogenesis through the secretion of growth factors, including IGF-1 and VEGF, which play critical roles in promoting the proliferation and differentiation of osteoblasts and neovascularization.[45-47] Consistent with previous studies, our study showed that the higher level of inflammatory factors (IL-6, IL-1β and TNF-α) and lower level of growth factors (IGF-1and VEGF) in the conditioned medium of TCPb group led to decreased osteogenic differentiation and was not conducive to the proliferation of mBMSCs. In brief, these results indicated that the secretion cytokines of macrophages modulated by surface topography of β-TCP in the early stage might contribute to β-TCP induced ectopic bone formation

and inappropriate immune regulatory cytokines could lead to severe inflammatory response which was detrimental to osteogenesis.

The final key point should be discussed is the possible mechanisms of the effect of surface topography on macrophages polarization. At first, the activation of STAT1 signal in macrophages is a crucial factor that regulates the polarization toward M1 phenotype [18, 48]and further increases the secretion of pro-inflammatory cytokines, such as TNF-α, IL-1β, IL-6. In particular, the inhibition of STAT1 could decrease the polarization of M1 in RAW 264.7 cells and further decrease the expression of pro-inflammatory genes.[49-50] WB results from our present study revealed that the phosphorylation level of STAT1 in RAW 264.7 cells cultured on TCPb significantly increased, suggesting that the polarization of macrophages toward to M1 phenotype may be regulated by the surface topography via STAT1 pathway. In addition, Integrin β 1 is a kind of cell surface receptor which binds to material surface protein. It mediates the signal transduction between cells and environment to regulate the behavior of macrophages and make cells respond to the environment.[51-52] A large number of studies have shown that integrin β1 was related to the activation of PI3k/Akt pathway which could contribute to enhance the activation of M2 macrophages while inhibit the activation of M1 macrophage.[53-56] In line with this, our present results showed that the level of integrin β1 and the phosphorylation levels of PI3K and Akt of RAW 264.7 cells cultured on the TCPs for 4 d were significantly elevated which was consistent with the higher expression of M2 secreted cytokines and lower expression of M1 secreted cytokines on TCPs. Collectively, these results indicated that the micron-surface topography of TCPb might induce macrophages into inflammatory state via STAT1 pathway while the sub-micron surface topography of TCPs might drive macrophages into a pro-healing state via PI3K/Akt pathway with combination with integrin β 1.

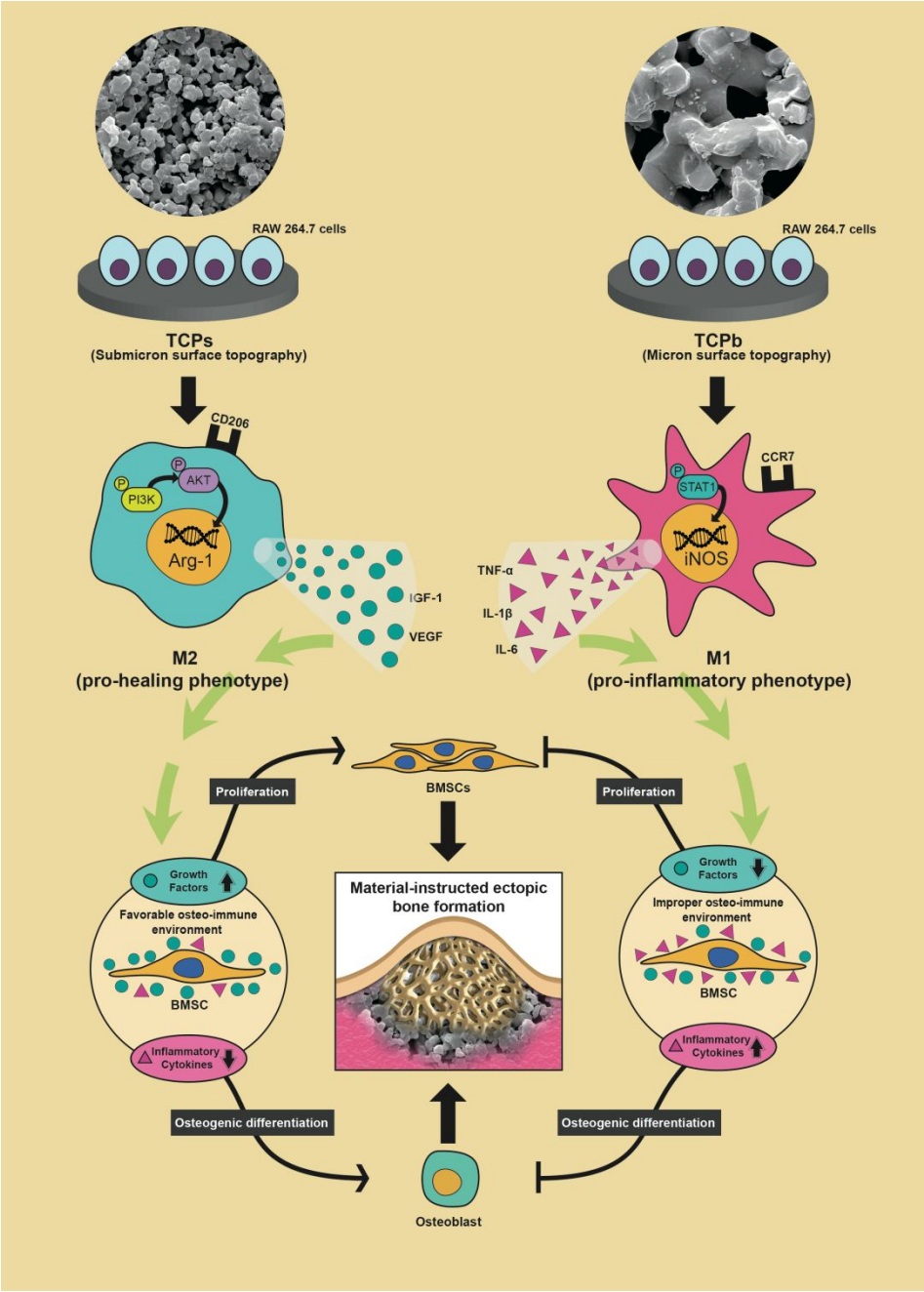

Figure 10. Summary of possible effects of surface topography on macrophages polarization and the roles of macrophages phenotypes in the process of material-instructed ectopic bone formation.

It should be noted that of all the physiochemical influence factors, only the surface topography of β-TCP was investigated in this study. However, besides surface topography, there

are other properties of biomaterials, including chemical composition and degradation properties have critical roles in ectopic bone formation. Therefore, future research will focus on other key properties to figure out the relationship between macrophage polarization and properties of materials to draw more comprehensive conclusions.

5. Conclusion

In summary, our results indicated that macrophages played an essential role in material-instructed ectopic bone formation. Furthermore, the macrophages polarization modulated by surface topography of β-TCP in the early stage is vital to material-instructed ectopic bone formation. Sub-micron surface topography of TCP ceramic can induce macrophages into a pro-healing state via PI3K/Akt pathway which can form favorable immune environment during the early period that is beneficial to the ectopic bone formation while micron surface topography of TCP ceramic could induce macrophages into an inflammatory state via STAT1 pathway which is detrimental to ectopic bone formation. The possible effects of surface topography on macrophages polarization and the roles of macrophages phenotypes in the process of material-instructed ectopic bone formation were summarized in Fig. 10.

ACKNOWLEDGMENT

This research was supported by the grants from The National Key Research and Development Program of China (grant number 2016YFC1102700), National Natural Science Foundation of China (grant number 81701027 and 81870814).

Reference

(1) Garcia-Gareta, E.; Coathup, M. J.; Blunn, G. W. Osteoinduction of bone grafting materials for bone repair and regeneration. *Bone* **2015,** *81*, 112-121.
(2) Habraken, W.; Habibovic, P.; Epple, M.; Bohner, M. Calcium phosphates in biomedical applications : materials for the future? *Materials Today* **2016,** *19* (2), 69–87.
(3) Malhotra, A.; Habibovic, P. Calcium Phosphates and Angiogenesis: Implications and Advances for Bone Regeneration. *Trends in biotechnology* **2016,** *34* (12), 983-992.
(4) Habibovic, P.; Yuan, H.; van den Doel, M.; Sees, T. M.; van Blitterswijk, C. A.; de Groot, K. Relevance of Osteoinductive Biomaterials in Critical-Sized Orthotopic Defect. *Journal of Orthopaedic Research* **2006,** *24* (5), 867-876.
(5) Duan, R.; Barbieri, D.; Luo, X.; Weng, J.; de Bruijn, J. D.; Yuan, H. Submicron-surface structured tricalcium phosphate ceramic enhances the bone regeneration in canine spine environment. *Journal of Orthopaedic Research* **2016,** *34* (11), 1865-1873.
(6) Yuan, H.; Fernandes, H.; Habibovic, P.; de Boer, J.; Barradas, A. M.; de Ruiter, A.; Walsh, W. R.; van Blitterswijk, C. A.; de Bruijn, J. D. Osteoinductive ceramics as a synthetic alternative to autologous bone grafting. *Proceedings of the National Academy of Sciences of the United States of America* **2010,** *107* (31), 13614-9.
(7) Bouler, J. M.; Pilet, P.; Gauthier, O.; Verron, E. Biphasic calcium phosphate ceramics for bone reconstruction: A review of biological response. *Acta biomaterialia* **2017,** *53*, 1-12.
(8) Samavedi, S.; Whittington, A. R.; Goldstein, A. S. Calcium phosphate ceramics in bone tissue engineering: a review of properties and their influence on cell behavior. *Acta biomaterialia* **2013,** *9* (9), 8037-45.
(9) Keselowsky, B. G.; Garcia, C. A. J. Surface chemistry modulates fibronectin conformation and directs integrin binding and specificity to control cell adhesion. *Journal of Biomedical Materials Research Part A B* **2003,** *66* (2), 247-259.
(10) Zhang, J.; Luo, X.; Barbieri, D.; Barradas, A. M.; de Bruijn, J. D.; van Blitterswijk, C. A.; Yuan, H. The size of surface microstructures as an osteogenic factor in calcium phosphate ceramics. *Acta biomaterialia* **2014,** *10* (7), 3254-63.
(11) Chen, Z.; Klein, T.; Murray, R. Z.; Crawford, R.; Chang, J.; Wu, C.; Xiao, Y. Osteoimmunomodulation for the development of advanced bone biomaterials. *Materials Today* **2016,** *19* (6), 304-321.
(12) Sridharan, R.; Cameron, A. R.; Kelly, D. J.; Kearney, C. J.; O'Brien, F. J. Biomaterial based modulation of macrophage polarization: a review and suggested design principles. *Materials Today* **2015,** *18* (6), 313-325.
(13) Chen, Z.; Bachhuka, A.; Han, S.; Wei, F.; Lu, S.; Visalakshan, R. M.; Vasilev, K.; Xiao, Y. Tuning Chemistry and Topography of Nanoengineered Surfaces to Manipulate Immune Response for Bone Regeneration Applications. *Acs Nano* **2017,** *11* (5), 4494-4506.
(14) Jin, S. S.; He, D. Q.; Luo, D.; Wang, Y.; Yu, M.; Guan, B.; Fu, Y.; Li, Z. X.; Zhang, T.; Zhou, Y. H.; Wang, C. Y.; Liu, Y. A Biomimetic Hierarchical Nanointerface Orchestrates Macrophage Polarization and Mesenchymal Stem Cell Recruitment To Promote Endogenous Bone Regeneration. *ACS Nano* **2019,** *13* (6), 6581-6595.
(15) Wang, M.; Chen, F.; Wang, J.; Chen, X.; Liang, J.; Yang, X.; Zhu, X.; Fan, Y.; Zhang, X. Calcium phosphate altered the cytokine secretion of macrophages and influenced the homing of mesenchymal stem cells. *Journal of Materials Chemistry B* **2018,** *6* (29), 4765-4774.

(16) Stout, R. D.; Jiang, C.; Matta, B.; Tietzel, I.; Watkins, S. K.; Suttles, J. Macrophages sequentially change their functional phenotype in response to changes in microenvironmental influences. *Journal of Immunology* **2005,** *175* (1), 342-349.
(17) Mills, C. D.; Kincaid, K.; Alt, J. M.; Heilman, M. J.; Hill, A. M. Pillars Article: M-1/M-2 Macrophages and the Th1/Th2 Paradigm. J. Immunol. 2000. 164: 6166-6173. *Journal of Immunology* **2017,** *199* (7), 2194.
(18) Mantovani, A.; Biswas, S. K.; Galdiero, M. R.; Sica, A.; Locati, M. Macrophage plasticity and polarization in tissue repair and remodelling. *Journal of Pathology* **2013,** *229* (2), 176-185.
(19) Brown, M. B.; Von, C. M.; Allam, A. B.; Reyes, L. M1/M2 macrophage polarity in normal and complicated pregnancy. *Front Immunol* **2014,** *5*, 606.
(20) Gordon, S. Alternative activation of macrophages. *Nature Reviews Immunology* **2003,** *3* (1), 23-35.
(21) Mosser, D. M.; Edwards, J. P. Exploring the full spectrum of macrophage activation. *Nature Reviews Immunology* **2008,** *8* (12), 958-969.
(22) Wynn, T. A.; Chawla, A.; Pollard, J. W. Macrophage biology in development, homeostasis and disease. *Nature* **2013,** *496* (7446), 445-455.
(23) Linda, V.; Baht, G. S.; Heather, W.; Adeline, N.; Qingxia, W.; Raymond, P.; Sivakami, M.; Marc, G.; Alman, B. A. Macrophages promote osteoblastic differentiation in-vivo: implications in fracture repair and bone homeostasis. *Journal of Bone & Mineral Research* **2015,** *30* (6), 1090-1102.
(24) Batoon, L.; Millard, S. M.; Wullschleger, M. E.; Preda, C.; Wu, A. C.; Kaur, S.; Tseng, H. W.; Hume, D. A.; Levesque, J. P.; Raggatt, L. J.; Pettit, A. R. CD169(+) macrophages are critical for osteoblast maintenance and promote intramembranous and endochondral ossification during bone repair. *Biomaterials* **2019,** *196*, 51-66.
(25) Davison, N. L.; Gamblin, A. L.; Layrolle, P.; Yuan, H.; de Bruijn, J. D.; Barrere-de Groot, F. Liposomal clodronate inhibition of osteoclastogenesis and osteoinduction by submicrostructured beta-tricalcium phosphate. *Biomaterials* **2014,** *35* (19), 5088-97.
(26) Zhang, W.; Zhao, F.; Huang, D.; Fu, X.; Li, X.; Chen, X. Strontium-substituted sub-micron bioactive glasses modulate macrophage responses for improved bone regeneration. *Acs Appl Mater Interfaces* **2016,** *8* (45), 30747.
(27) Rooijen, N. v.; Kesteren-Hendrikx, E. v. " In Vivo " Depletion of Macrophages by Liposome-Mediated "Suicide". *Methods Enzymol* **2003,** *373* (373), 3-16.
(28) Gamblin, A. L.; Brennan, M. A.; Renaud, A.; Yagita, H.; Lezot, F.; Heymann, D.; Trichet, V.; Layrolle, P. Bone tissue formation with human mesenchymal stem cells and biphasic calcium phosphate ceramics: the local implication of osteoclasts and macrophages. *Biomaterials* **2014,** *35* (36), 9660-7.
(29) Folkman, J.; Moscona, A. Role of cell shape in growth control. *Nature* **1978,** *273* (5661), 345-9.
(30) Chen, S.; Jones, J. A.; Xu, Y.; Low, H. Y.; Anderson, J. M.; Leong, K. W. Characterization of topographical effects on macrophage behavior in a foreign body response model. *Biomaterials* **2010,** *31* (13), 3479-91.
(31) Mcwhorter, F. Y.; Tingting, W.; Phoebe, N.; Thanh, C.; Liu, W. F. Modulation of macrophage phenotype by cell shape. *Proceedings of the National Academy of Sciences of the United States of America* **2013,** *110* (43), 17253-17258.

(32) Chen, Z.; Ni, S.; Han, S.; Crawford, R.; Lu, S.; Wei, F.; Chang, J.; Wu, C.; Xiao, Y. Nanoporous microstructures mediate osteogenesis by modulating the osteo-immune response of macrophages. *Nanoscale* **2016,** *9* (2), 706.
(33) Lee, S.; Choi, J.; Shin, S.; Im, Y. M.; Song, J.; Kang, S. S.; Nam, T. H.; Webster, T. J.; Kim, S. H.; Khang, D. Analysis on migration and activation of live macrophages on transparent flat and nanostructured titanium. *Acta biomaterialia* **2011,** *7* (5), 2337-44.
(34) Ma, Q. L.; Zhao, L. Z.; Liu, R. R.; Jin, B. Q.; Song, W.; Wang, Y.; Zhang, Y. S.; Chen, L. H.; Zhang, Y. M. Improved implant osseointegration of a nanostructured titanium surface via mediation of macrophage polarization. *Biomaterials* **2014,** *35* (37), 9853-9867.
(35) Edin, S.; Wikberg, M. L.; Rutegård, J.; Oldenborg, P. A.; Palmqvist, R. Phenotypic Skewing of Macrophages In Vitro by Secreted Factors from Colorectal Cancer Cells. *Plos One* **2013,** *8* (9), e74982.
(36) Rossol, M.; Pierer, M.; Raulien, N.; Quandt, D.; Meusch, U.; Rothe, K.; Schubert, K.; Schöneberg, T.; Schaefer, M.; Krügel, U. Extracellular Ca2+ is a danger signal activating the NLRP3 inflammasome through G protein-coupled calcium sensing receptors. *Nature communications* **2012,** *3*, 1329.
(37) Chen, Z.; Wu, C.; Gu, W.; Klein, T.; Crawford, R.; Xiao, Y. Osteogenic differentiation of bone marrow MSCs by beta-tricalcium phosphate stimulating macrophages via BMP2 signalling pathway. *Biomaterials* **2014,** *35* (5), 1507-18.
(38) Fearing, B. V.; Dyke, M. E. V. In vitro response of macrophage polarization to a keratin biomaterial. *Acta biomaterialia* **2014,** *10* (7), 3136-3144.
(39) Zhenyu, Q. The use of THP-1 cells as a model for mimicking the function and regulation of monocytes and macrophages in the vasculature. *Atherosclerosis* **2012,** *221* (1), 2-11.
(40) Tidball, J. G. Inflammatory processes in muscle injury and repair. *American Journal of Physiology-Regulatory, Integrative and Comparative Physiology* **2005,** *288* (2), R345-R353.
(41) Klopfleisch, R. Macrophage reaction against biomaterials in the mouse model – phenotypes, functions and markers. *Acta biomaterialia* **2016,** *43*, 3-13.
(42) Lin, G.; Ding, Z.; Hu, R.; Wang, X.; Chen, Q.; Zhu, X.; Liu, K.; Liang, J.; Lu, F.; Lei, D. Cytotoxicity and immune response of CdSe/ZnS Quantum dots towards a murine macrophage cell line. *Rsc Advances* **2014,** *4* (11), 5792-5797.
(43) Zhou, F. H.; Foster, B. K.; Zhou, X. F.; Cowin, A. J.; Xian, C. J. TNF-alpha mediates p38 MAP kinase activation and negatively regulates bone formation at the injured growth plate in rats. *Journal of Bone & Mineral Research* **2010,** *21* (7), 1075-1088.
(44) Alhamdi, J. R.; Peng, T.; Al-Naggar, I. M.; Hawley, K. L.; Spiller, K. L.; Kuhn, L. T. Controlled M1-to-M2 transition of aged macrophages by calcium phosphate coatings. *Biomaterials* **2018**, S0142961218304897.
(45) Pajarinen, J.; Lin, T.; Gibon, E.; Kohno, Y.; Maruyama, M.; Nathan, K.; Lu, L.; Yao, Z.; Goodman, S. B. Mesenchymal Stem Cell-Macrophage Crosstalk and Bone Healing. *Biomaterials* **2018,** *196*, S0142961217308347.
(46) Jetten, N.; Verbruggen, S.; Gijbels, M. J.; Post, M. J.; Winther, M. P. J. D.; Donners, M. M. P. C. Anti-inflammatory M2, but not pro-inflammatory M1 macrophages promote angiogenesis in vivo. *Angiogenesis* **2014,** *17* (1), 109-118.
(47) Gong, L.; Zhao, Y.; Zhang, Y.; Ruan, Z. The Macrophage Polarization Regulates MSC Osteoblast Differentiation in vitro. *Annals of Clinical & Laboratory Science* **2016,** *46* (1), 65.
(48) Lawrence, T.; Natoli, G. Transcriptional regulation of macrophage polarization: enabling diversity with identity. *Nature Reviews Immunology* **2011,** *11* (11), 750-61.

(49) Wager, C. M. L.; Hole, C. R.; Wozniak, K. L.; Olszewski, M. A.; Mueller, M.; Jr, F. L. W. STAT1 Signaling within Macrophages Is Required for Antifungal Activity against Cryptococcus neoformans. *Infection & Immunity* **2015,** *83* (12), 4513-27.
(50) Gan, Z. S.; Wang, Q. Q.; Li, J. H.; Wang, X. L.; Wang, Y. Z.; Du, H. H. Iron Reduces M1 Macrophage Polarization in RAW264.7 Macrophages Associated with Inhibition of STAT1. *Mediators of Inflammation* **2017,** *2017* (10), 1-9.
(51) Delon, I.; Brown, N. H. Integrins and the actin cytoskeleton. *Current Opinion in Cell Biology* **2007,** *19* (1), 43-50.
(52) Giancotti, F. G.; Ruoslahti, E. Integrin signaling. *Science* **1999,** *285* (5430), 1028-1032.
(53) Rauh, M. J.; Ho, V.; Pereira, C.; Sham, A.; Sly, L. M.; Lam, V.; Huxham, L.; Minchinton, A. I.; Mui, A.; Krystal, G. SHIP represses the generation of alternatively activated macrophages. *Immunity* **2005,** *23* (4), 361-374.
(54) Araki, K.; Ellebedy, A. H.; Ahmed, R. TOR in the immune system. *Current Opinion in Cell Biology* **2011,** *23* (6), 707-715.
(55) Kianoush, F.; Nematollahi, M.; Waterfield, J. D.; Brunette, D. M. Regulation of RAW264.7 Macrophage Polarization on Smooth and Rough Surface Topographies by Galectin-3. *Journal of Biomedical Materials Research Part A* **2017,** *105*.
(56) Lv, L.; Xie, Y.; Li, K.; Hu, T.; Lu, X.; Cao, Y.; Zheng, X. Unveiling the Mechanism of Surface Hydrophilicity-Modulated Macrophage Polarization. *Adv Healthc Mater* **2018,** *7* (19), e1800675.

Graphic Abstract